Polarization of supported graphene by slowly moving charges

I. Radović and Lj. Hadžievski
VINČA Institute of Nuclear Sciences, P.O. Box 522, 11001 Belgrade, Serbia

Z. L. Mišković*
Department of Applied Mathematics, University of Waterloo, Waterloo, Ontario, Canada N2L 3G1
(Received 23 October 2007; published 26 February 2008)

We describe the dynamic polarization of graphene's π electrons by means of the Vlasov equations in the relaxation-time approximation and evaluate the stopping and the image forces on slow ions moving parallel to a supported graphene under the gating conditions. While the effects of temperature and the gate potential on these forces are conveniently included by means of a single scaling parameter, the effects of variation in size of the gap between graphene and the SiO_2 substrate are found to be quite large, pointing to the need for including this gap explicitly in modeling of polarization of graphene.

DOI: 10.1103/PhysRevB.77.075428 PACS number(s): 79.20.Rf, 34.50.Bw, 34.35.+a

I. INTRODUCTION

Ever since stable graphene was isolated,[1] its peculiar electron transport properties have attracted a great deal of interest.[2] One currently witnesses a surge of theoretical accounts of these properties, especially regarding the so-called minimum conductivity.[3–6] One of the important contributions to the conductivity of graphene comes from electron scattering on charged impurities, which are ubiquitous in graphene and its surrounding. Therefore, much attention is being devoted to studying the screening of such impurities by polarization of charge carriers in graphene in the static regime, within both linear[3–6] and nonlinear models.[7] On the other hand, dynamic polarization of graphene opens a range of possible application areas,[8] including the emerging field of plasmonics.[9] Namely, recent investigations of the low-energy collective or plasma excitations of graphene electrons show that this material may be used as a basis for nanoelectronic devices operating in the terahertz range of frequencies.[7,10–16]

In this paper, we analyze the dynamic screening of external charges moving nearby supported graphene under the gating conditions. Unlike our previous study of interactions of fast particles with graphene,[17] we are interested here in relatively slow ions, moving in the range of speeds from around Bohr velocity down to thermal speeds. In this regime, the dynamic response of graphene is dominated by the peculiar behavior of the low-energy excitations of its π electrons which may be treated as a two-dimensional gas of the massless Dirac fermions.[8] There are several possible domains of interest for such study, ranging from chemisorption of alkali-metal atoms on graphene[18] to the friction of migrating atoms and molecules,[19,20] which can be used to study viscosity of fluids moving near graphene, to various phenomena involving the low-energy ion-surface scattering.[21] Moreover, the directional effects in ion interactions with graphene-based materials have been studied in the context of low-energy ion channeling through carbon nanotubes,[22] as well as in the context of ion interactions with highly oriented pyrolytic graphite, including implantation,[23] channeling,[24] and ion-induced secondary electron emission from this target.[25] Most of such scattering configurations involve ion impacts upon graphene surface under grazing incidence, and it is tempting to speculate about further interesting parallels with the phenomenology discovered in the area of grazing scattering of particles from solid surfaces.[26] With a view of extending such studies of solid surfaces to graphene, we explore here the effects of dynamic-polarization forces on ions moving parallel to a single layer of supported graphene. Specifically, we calculate the stopping force and the image force which describe, respectively, the rate of dissipation of ion's kinetic energy into both single-particle and collective electron excitations in graphene, and the effects of the image potential V_i, which attracts the ion toward graphene while elevating its bound-electron orbital energies.[27]

Graphene usually appears in experimental situations as supported by a substrate[28,29] which may exert quite strong influence on its dynamic polarization, as was discussed recently for the cases of fast ions moving in carbon nanotubes[30] or over a supported graphene.[17] While the configuration of graphene on metal[28] opens interesting possibility of exciting novel modes of collective electron excitations due to plasmon hybridization,[30,31] we limit ourselves here to studying the effects of an insulating substrate, such as SiO_2 having a dielectric constant of $\epsilon_{sub} \approx 3.9$. Interestingly, while Ishigami *et al.*[29] have found that the distance h between graphene and substrate is on the order of the distance between graphene layers in graphite or even larger, the effects of finite h were invariably ignored in all previous theoretical studies of screening by graphene.[3–7,10–16] In those studies, it was usually assumed that there is a background dielectric constant having the value which is "the average of that of the substrate… and that of the vacuum due to the image effect,"[3] giving $(\epsilon_{sub}+1)/2 \approx 2.45$ for SiO_2. As it will be shown below, this assumption amounts to taking a zero gap, $h=0$, between graphene and substrate, so that we make one of our principal goals to demonstrate just how strong are the effects of finite h in the dynamic-polarization forces on moving ions, implying a need to include the gap size explicitly in modeling of other screening phenomena by graphene.

In our previous work,[17] we studied the dynamic screening of fast ions and molecules due to the collective excitations of both π and σ electrons in graphene, which can be conveniently described by a two-fluid hydrodynamic model[30] for

particle speeds above the so-called kinematic threshold for plasmon excitation being on the order of the Bohr velocity for carbon valence electrons. Here, however, we are interested in slow ions, moving at the speeds under Bohr's velocity, so that the dynamic response of graphene is dominated by the single-particle and collective excitations of its π electrons, whereas σ electrons are not excited owing to their having a large band gap. Such low-energy excitations require going beyond the hydrodynamic model, and the dielectric-response theory for surfaces and layered structures[32] is a convenient way to proceed, given that the dielectric function for graphene is available within the random phase approximation (RPA) based on a linear approximation for the π electron bands.[7,10,12] However, we shall describe here the dynamic response of the graphene and/or substrate system by means of a semiclassical Vlasov equation for graphene's π electrons, which was used recently by Ryzhii *et al.*[15] to deduce a low-frequency plasmon dispersion for such system. The main shortcoming of the semiclassical approach compared to the RPA formalism is the absence of high-energy interband electron transitions, which will not be so critical for our study in the case of a sufficiently large gate voltage and for slow ions moving at sufficiently high distances from the graphene plane. On the other hand, the relative simplicity of the semiclassical approach to dynamic screening in comparison to the RPA results allows for a straightforward inclusion of finite temperatures, as well as for an easy treatment of the finite gap between the graphene and substrate. While our results for the dynamic-polarization forces conveniently include the effects of temperature, along with the gate voltage, through a single scaling parameter, the role of the graphene-substrate gap will be examined in detail as an external parameter. Further, among other advantages of the semiclassical approach, explored here, is the explicit inclusion of various electron scattering processes in the Vlasov equation within the relaxation-time approximation, making it compatible with calculations of the graphene conductivity based on the Boltzmann theory,[3,4] whereas electron collisions have yet to be included in the RPA results for graphene, e.g., by means of Mermin's method.[33] Finally, it will be shown here that a steady-state solution of the Vlasov equation provides a natural framework for deriving a fully self-consistent, temperature-dependent nonlinear Thomas–Fermi (TF) model for static screening of charged impurities in or near the supported graphene under arbitrary gating conditions.[7]

After outlining the theory used to treat the effects of substrate and to deduce a model dielectric function from the Vlasov equation, we shall discuss the results for the stopping and image forces for a range of the relevant parameters. Our concluding remarks will be followed by a derivation of the nonlinear model for static screening in Appendix. We shall use the Gaussian cgs units and denote the charge of a proton by $e>0$.

II. BASIC THEORY

A. Effects of substrate

We use a Cartesian coordinate system with coordinates $\{\mathbf{r},z\}$, where $\mathbf{r}=\{x,y\}$, and assume that graphene is placed in the $z=0$ plane. A substrate with dielectric constant ϵ_{sub} is assumed to occupy the region $z\leqslant -h$ underneath the graphene, whereas the region $z>-h$ is assumed to be vacuum or air. The ground state of such system under the gating conditions is characterized by certain (uniform) charge densities induced on both graphene and the substrate surface. When a point charge Q moves parallel to graphene at a fixed position $z_0>0$ above it with a constant velocity $\mathbf{v}=\{v_x,v_y\}$, so that its density can be written as $\rho_{\text{ext}}(\mathbf{r},z,t)=Q\delta(\mathbf{r}-\mathbf{v}t)\delta(z-z_0)$, then the resulting electric potential $\Phi_{\text{ext}}(\mathbf{r},z,t)$ will perturb the system giving rise to deviations from the ground-state charge densities (per unit area) on both the graphene and substrate surface which we denote, respectively, by $\sigma_{\text{gr}}(\mathbf{r},t)$ and $\sigma_{\text{sub}}(\mathbf{r},t)$.

Next, we resort to the method of Doerr and Yu[34] to treat the effects of substrate, assuming its surface to be structureless. Denoting the electric potentials due to the induced charge densities σ_{gr} and σ_{sub}, respectively, by $\Phi_{\text{gr}}(\mathbf{r},z,t)$ and $\Phi_{\text{sub}}(\mathbf{r},z,t)$, the total (screened) electric potential in the system, Φ, can be written as

$$\Phi=\Phi_{\text{ext}}+\Phi_{\text{gr}}+\Phi_{\text{sub}}. \tag{1}$$

Then, if there are no free charges on the substrate surface (such as, e.g., dopant centers), one can use the continuity of the normal component of the displacement vector,

$$\left.\frac{\partial\Phi}{\partial z}\right|_{z=-h+0}=\epsilon_{\text{sub}}\left.\frac{\partial\Phi}{\partial z}\right|_{z=-h-0}, \tag{2}$$

to obtain σ_{sub}.[17,30,34] This is easily implemented by using the Fourier transform with respect to time, $t\rightarrow\omega$, and coordinates in the xy plane, $\mathbf{r}\rightarrow\mathbf{k}$, defined by

$$A(\mathbf{r},z,t)=\int\frac{d^2\mathbf{k}}{(2\pi)^2}\int\frac{d\omega}{2\pi}e^{i\mathbf{k}\cdot\mathbf{r}-i\omega t}\tilde{A}(\mathbf{k},z,\omega)$$

for an arbitrary function A. Thus, the Fourier transformed components of the electric potential in Eq. (1) are given by

$$\tilde{\Phi}_{\text{ext}}(\mathbf{k},z,\omega)=2\pi Q\delta(\omega-\mathbf{k}\cdot\mathbf{v})\frac{2\pi}{k}e^{-k|z-z_0|}, \tag{3}$$

$$\tilde{\Phi}_{\text{gr}}(\mathbf{k},z,\omega)=\frac{2\pi}{k}e^{-k|z|}\tilde{\sigma}_{\text{gr}}(\mathbf{k},\omega), \tag{4}$$

$$\tilde{\Phi}_{\text{sub}}(\mathbf{k},z,\omega)=\frac{2\pi}{k}e^{-k|z+h|}\tilde{\sigma}_{\text{sub}}(\mathbf{k},\omega), \tag{5}$$

where $k=\sqrt{k_x^2+k_y^2}$.

Finally, we note that, for a self-consistent determination of the total electric potential Φ, one only requires the polarization function of graphene, $\chi(\mathbf{k},\omega)$, which gives $\sigma_{\text{gr}}=-en_{\text{gr}}$ in terms of the induced number density per unit area of electrons on graphene, defined by

$$\tilde{n}_{\text{gr}}(\mathbf{k},\omega)=\chi(\mathbf{k},\omega)\tilde{\Phi}(\mathbf{k},z,\omega)|_{z=0}. \tag{6}$$

Using the relation [Eq. (6)] along with [Eqs. (3)–(5)] and the Fourier transforms of the boundary condition [Eq. (2)] and the decomposition of the total potential [Eq. (1)], one can

obtain the Fourier transform of the induced potential, $\Phi_{\rm ind}=\Phi_{\rm sub}+\Phi_{\rm gr}$, in the region above graphene ($z>0$), as follows:

$$\tilde{\Phi}^{>}_{\rm ind}(\mathbf{k},z,\omega)=2\pi Q\delta(\omega-\mathbf{k}\cdot\mathbf{v})\frac{2\pi}{k}e^{-k(z+z_0)}\left[\frac{1}{\epsilon(\mathbf{k},\mathbf{k}\cdot\mathbf{v})}-1\right], \tag{7}$$

where

$$\epsilon(\mathbf{k},\omega)=\epsilon_0(k)+\frac{2\pi e}{k}\chi(\mathbf{k},\omega) \tag{8}$$

is the dielectric function of supported graphene, with

$$\epsilon_0(k)\equiv\frac{\epsilon_{\rm sub}+1}{2}\frac{1+\coth(kh)}{\epsilon_{\rm sub}+\coth(kh)} \tag{9}$$

being the background dielectric function which quantifies the effects of substrate on the response of graphene. Note that $\epsilon_0(k)$ takes the values in the range between 1 and $(\epsilon_{\rm sub}+1)/2$, characterizing, respectively, the case of a *free* graphene ($h\to\infty$) and the case of a *zero gap* ($h=0$) between the graphene and substrate, which is usually considered in the literature.

As before,[17,30] the stopping and the image forces on the moving charge are defined in terms of the induced potential, $\Phi^{>}_{\rm ind}(\mathbf{r},z,t)$, respectively, as follows:

$$F_s=-Q\hat{\mathbf{v}}\cdot\frac{\partial}{\partial\mathbf{r}}\Phi^{>}_{\rm ind}\Big|_{\mathbf{r}=\mathbf{v}t,z=z_0}, \tag{10}$$

where $\hat{\mathbf{v}}=\mathbf{v}/v$, and

$$F_i=-Q\frac{\partial}{\partial z}\Phi^{>}_{\rm ind}\Big|_{\mathbf{r}=\mathbf{v}t,z=z_0}. \tag{11}$$

We finally note that a similar procedure can be repeated for a projectile moving between the graphene and substrate ($-h<z_0<0$), in which case one would evaluate the stopping and image forces from an expression for the induced potential $\tilde{\Phi}^{<}_{\rm ind}$, valid in the region underneath the graphene ($z<0$), which is slightly more complex than Eq. (7).

B. Model dielectric function of graphene

We shall treat graphene assuming a uniform two-dimensional background of positive ion cores. Let us first consider the ground state of graphene with an equilibrium charge density per unit area, $-en_0$, induced by applying a gate voltage V_g underneath the substrate layer of thickness $w_{\rm sub}\gg h$, so that

$$n_0=\frac{\epsilon_{\rm sub}}{4\pi e}\frac{V_g}{w_{\rm sub}} \tag{12}$$

from elementary electrostatics.[15] On the other hand, the equilibrium number density of charge carriers per unit area is given by

$$n_0=\int_0^\infty d\varepsilon\rho_+(\varepsilon)f(\varepsilon)-\int_{-\infty}^0 d\varepsilon\rho_-(\varepsilon)[1-f(\varepsilon)], \tag{13}$$

where

$$\rho_\pm(\varepsilon)=\pm\frac{g_d\varepsilon}{2\pi(\hbar v_F)^2}H(\pm\varepsilon), \tag{14}$$

with $H(\varepsilon)$ being the standard unit-step Heaviside function, are the electron energy densities in the conduction and valence bands, respectively. Here, the degeneracy factor, $g_d=4$, and the Fermi speed of graphene, $v_F\approx c/300$ (c being the speed of light) characterize the band structure of π electrons in the approximation of linear dispersion, $\varepsilon_\pm(\mathbf{p})=\pm v_F p$, where $\mathbf{p}$ is the electron quasimomentum and p its magnitude. Using the Fermi-Dirac distribution,

$$f(\varepsilon)=\frac{1}{1+\exp[(\varepsilon-\mu)/k_BT]}, \tag{15}$$

in Eq. (13) allows one to express n_0 as a function of the chemical potential,

$$n_0(\mu)=\frac{g_d}{2\pi}\left(\frac{k_BT}{\hbar v_F}\right)^2[\mathrm{dilog}(1+e^{-\mu/k_BT})-\mathrm{dilog}(1+e^{\mu/k_BT})], \tag{16}$$

where dilog is the standard dilogarithm function.[35] Inverting the relation [Eq. (16)] can be used in conjunction with Eq. (12) to deduce the value of chemical potential μ for any applied gate voltage V_g. Clearly, in the ungated situation (i.e., for intrinsic graphene), one has $n_0=0$ and consequently $\mu=0$, whereas the zero-temperature limit, $T\to 0$ (and, accordingly, $\mu\to\varepsilon_F$), amounts to the relation $n_0=\frac{g_d}{4\pi}\left(\frac{\varepsilon_F}{\hbar v_F}\right)^2\mathrm{sgn}(\varepsilon_F)$, where the Fermi energy ε_F is often used to define the Fermi momentum of graphene by $p_F=|\varepsilon_F|/v_F$.

In order to analyze the dynamic response of π electrons in graphene, we use the approach of Ryzhii *et al.*[15] based on the Vlasov-type equations for the probability density functions $f_\pm(\mathbf{p},\mathbf{r},t)$ of graphene's π electrons in the conduction and valence bands,

$$\frac{\partial f_\pm}{\partial t}+\mathbf{v}_\pm(\mathbf{p})\cdot\frac{\partial f_\pm}{\partial\mathbf{r}}+\mathbf{F}_t(\mathbf{r},t)\cdot\frac{\partial f_\pm}{\partial\mathbf{p}}=J_\pm, \tag{17}$$

where $\mathbf{v}_\pm(\mathbf{p})\equiv\partial\varepsilon_\pm(\mathbf{p})/\partial\mathbf{p}=\pm v_F\hat{\mathbf{p}}$, with $\hat{\mathbf{p}}=\mathbf{p}/p$, and

$$\mathbf{F}_t(\mathbf{r},t)=e\frac{\partial}{\partial\mathbf{r}}\Phi(\mathbf{r},z,t)\Big|_{z=0} \tag{18}$$

is a tangential force on an electron in the graphene plane due to the total electric potential Φ in the system. We shall consider the Vlasov equations [Eq. (17)] in the relaxation-time approximation by writing the collision terms as

$$J_\pm=-\frac{f_\pm-f^0_\pm}{\tau(\mathbf{p})}, \tag{19}$$

where $f^0_\pm(\mathbf{p},\mathbf{r})$ are stationary (unperturbed) solutions of Eq. (17). While we shall be primarily concerned with the collisionless case [Eq. (17)] by taking the limit of a vanishing decay constant, $\gamma=\tau^{-1}\to 0^+$, we note that various mechanisms of electron scattering can be easily incorporated in the Vlasov equation by using the available expressions for the relaxation time $\tau(\mathbf{p})$, which are currently under investigation within the framework of the Boltzmann theory of graphene

conductivity.[3–5] Note that the connection with the Poisson equation for electric potential is achieved by using the induced density (per unit area) of charge carriers on graphene, $n_{\rm gr}(\mathbf{r},t)=n(\mathbf{r},t)-n_0$, defined by

$$n_{\rm gr}(\mathbf{r},t) = g_d \int \frac{d^2\mathbf{p}}{(2\pi\hbar)^2}[\delta f_+(\mathbf{p},\mathbf{r},t) + \delta f_-(\mathbf{p},\mathbf{r},t)], \quad (20)$$

where $\delta f_\pm \equiv f_\pm(\mathbf{p},\mathbf{r},t)-f[\varepsilon_\pm(\mathbf{p})]$.

We further assume that the potential Φ presents a weak perturbation of the ground state described by the Fermi-Dirac distribution, $f_\pm^0(\mathbf{p},\mathbf{r})=f[\varepsilon_\pm(\mathbf{p})]$, and therefore truncate the expansion $f_\pm=f_\pm^0+\delta f_\pm+\cdots$ after the first term. On applying the Fourier transform with respect to t and $\mathbf{r}$, one obtains the linearized Vlasov equations for the perturbations of the probability densities, $\widetilde{\delta f_\pm}(\mathbf{p},\mathbf{k},\omega)$, as follows:

$$-i\omega\widetilde{\delta f_\pm} + i\mathbf{k}\cdot\mathbf{v}_\pm(\mathbf{p})\widetilde{\delta f_\pm} + i\mathbf{k}\cdot\mathbf{v}_\pm(\mathbf{p})f'[\varepsilon_\pm(\mathbf{p})] \times e\widetilde{\Phi}(\mathbf{k},z,\omega)|_{z=0} = -\gamma(\mathbf{p})\widetilde{\delta f_\pm}, \quad (21)$$

where $f'(\varepsilon)=df(\varepsilon)/d\varepsilon$. Finally, solving Eq. (21) for $\widetilde{\delta f_\pm}$ and substituting into the Fourier transformed relation [Eq. (20)] allow one to refer to the definition [Eq. (6)] and write the polarization function of graphene as $\chi=\chi_+ + \chi_-$, where

$$\chi_\pm(k,\omega) = \frac{eg_d}{(2\pi\hbar)^2}\int d^2\mathbf{p} f'[\varepsilon_\pm(\mathbf{p})]\frac{\mathbf{k}\cdot\mathbf{v}_\pm(\mathbf{p})}{\omega + i\gamma(\mathbf{p}) - \mathbf{k}\cdot\mathbf{v}_\pm(\mathbf{p})}. \quad (22)$$

A useful intermediate result can be written when γ depends only on the magnitude of the electron quasimomentum,

$$\chi(k,\omega) = e\int_{-\infty}^{\infty} d\varepsilon\rho(\varepsilon)f'(\varepsilon)\int_{-\pi}^{\pi}\frac{d\theta}{2\pi}\frac{kv_F\cos\theta}{\omega + i\gamma[p(\varepsilon)] - kv_F\cos\theta}, \quad (23)$$

where $\rho(\varepsilon)\equiv\rho_+(\varepsilon)+\rho_-(\varepsilon)=\frac{g_d|\varepsilon|}{2\pi(\hbar v_F)^2}$ is the total energy density of the π-electron bands and $p(\varepsilon)=|\varepsilon|/v_F$. After some algebra, the integral over θ in Eq. (23) amounts to an expression $-1+\mathcal{X}(\omega,k;\gamma)$, where the real and the imaginary parts, $\mathcal{X}_r$ and $\mathcal{X}_i$, of the auxiliary function $\mathcal{X}(\omega,k;\gamma)$ are, respectively, even and odd functions of ω and are given for $\omega>0$ by

$$\mathcal{X}_r(\omega,k;\gamma) = \frac{\Omega\sqrt{A+\sqrt{A^2+B^2}} + \Gamma\sqrt{-A+\sqrt{A^2+B^2}}}{\sqrt{2(A^2+B^2)}}, \quad (24)$$

$$\mathcal{X}_i(\omega,k;\gamma) = \frac{\Gamma\sqrt{A+\sqrt{A^2+B^2}} - \Omega\sqrt{-A+\sqrt{A^2+B^2}}}{\sqrt{2(A^2+B^2)}}. \quad (25)$$

Here, $A=\Omega^2-\Gamma^2-1$ and $B=2\Omega\Gamma$, with $\Omega=\omega/(kv_F)$ and $\Gamma=\gamma/(kv_F)$, indicating that $\mathcal{X}_r$ and $\mathcal{X}_i$ are, in fact, universal functions of Ω and Γ.

If one can further assume $\gamma\approx$const, e.g., by taking $\gamma(p)\approx\gamma(p_F)$ in the low temperature case, then the integral over ε in Eq. (23) can be completed, giving simply $-\partial n_0(\mu)/\partial\mu$, where $n_0(\mu)$ is given by Eq. (16). Finally, the dielectric function of the supported graphene is obtained from Eq. (8) as follows:

$$\epsilon(k,\omega) = \epsilon_0(k) + \frac{k_{\rm TF}}{k}[1-\mathcal{X}_r(\omega,k;\gamma) - i\mathcal{X}_i(\omega,k;\gamma)], \quad (26)$$

where we have defined the TF inverse screening length by

$$k_{\rm TF} \equiv 2\pi e^2\frac{\partial n_0}{\partial\mu} = g_d e^2\frac{k_BT}{(\hbar v_F)^2}\ln\left\{2\left[1+\cosh\left(\frac{\mu}{k_BT}\right)\right]\right\}, \quad (27)$$

having the zero-temperature limit of $k_{\rm TF}\to g_d e^2|\varepsilon_F|/(\hbar v_F)^2 \approx 10p_F/\hbar$.

It is worthwhile analyzing the dielectric function [Eq. (26)] in some detail. In the collisionless limit, one obtains from Eqs. (24) and (25) simply

$$\mathcal{X}_r(\omega,k) = \frac{|\omega|}{\sqrt{\omega^2-(kv_F)^2}}H[\omega^2-(kv_F)^2], \quad (28)$$

$$\mathcal{X}_i(\omega,k) = -\frac{\omega}{\sqrt{(kv_F)^2-\omega^2}}H[(kv_F)^2-\omega^2], \quad (29)$$

showing that there exists a continuum of single-particle excitations for $0<\omega<kv_F$ corresponding to the intraband electron transitions, whereas the real root of $\epsilon(k,\omega)=0$ implies that there are plasmon excitations in the high-frequency region $\omega>kv_F$, with the dispersion $\omega=\omega_p(k)$ defined by

$$\omega_p(k) = v_F[k+\mathsf{k}_{\rm TF}(k)]\sqrt{\frac{k}{k+2\mathsf{k}_{\rm TF}(k)}}, \quad (30)$$

where $\mathsf{k}_{\rm TF}(k)\equiv k_{\rm TF}/\epsilon_0(k)$ is the screened, wave-number dependent TF inverse screening length. In the limit of a zero gap between the graphene and substrate, one has $\mathsf{k}_{\rm TF}=2k_{\rm TF}/(\epsilon_{\rm sub}+1)=$const, giving the familiar long-wavelength limit, $\omega_p(k)\sim\sqrt{k}$, typical of a two-dimensional electron gas. By further considering the low-frequency and the long-wavelength limits in Eq. (28) and (29), one can see that the dielectric function of the supported graphene obtained here reproduces, at least qualitatively, both the collective and intraband electron excitations in the dielectric function obtained from a full RPA,[7,10,12] while the interband electron excitations stemming from the Pauli exclusion principle are not reproduced in the present semiclassical theory. However, since the interband electron transitions yield a high-frequency continuum in the region $\omega>\omega_F+|v_Fk-\omega_F|$, where $\omega_F\equiv|\varepsilon_F|/\hbar$, one expects that at least the low-frequency and the long-wavelength electron excitations will be correctly approximated by the present model. As far as the stopping and image forces, Eqs. (10) and (11), are concerned, it follows from the exponential in Eq. (7) that the contributions of wavelengths shorter than $\sim z_0$ will be suppressed anyway. Taking further into account the kinematic constraint $\omega=\mathbf{k}\cdot\mathbf{v}$ in Eq. (7), one may ascertain that the results based on the Vlasov equations will be adequate for slow ions moving far

enough from a graphene layer exposed to a sufficiently large gate voltage.

Moreover, it also follows from Eqs. (28) and (29) that, in the static case, we obtain the standard TF dielectric function without the effects of collisions,

$$\epsilon(k) = \epsilon_0(k) + k_{\mathrm{TF}}/k, \tag{31}$$

which has been used elsewhere with the assumption $\epsilon_0(k) = \text{const}$.[3–5] However, the static limit in Eqs. (24) and (25) already gives a different result for the dielectric function with finite γ, namely,

$$\epsilon(k) = \epsilon_0(k) + \frac{k_{\mathrm{TF}}}{k}\left[1 - \frac{\gamma}{\sqrt{\gamma^2 + (kv_F)^2}}\right], \tag{32}$$

which is not reproduced by the standard RPA approach.

III. RESULTS FOR STOPPING AND IMAGE FORCES

Using the definitions [Eqs. (10) and (11)], one obtains, respectively, the stopping and image forces as follows:

$$F_s = \frac{2}{\pi}\frac{Q^2}{v}\int_0^\infty dk e^{-2kz_0}\int_0^{kv} d\omega \frac{\omega}{\sqrt{k^2v^2 - \omega^2}}\,\mathrm{Im}\left[\frac{1}{\epsilon(k,\omega)}\right], \tag{33}$$

$$F_i = \frac{2}{\pi}Q^2\int_0^\infty dk k e^{-2kz_0}\int_0^{kv} \frac{d\omega}{\sqrt{k^2v^2 - \omega^2}}\,\mathrm{Re}\left[\frac{1}{\epsilon(k,\omega)} - 1\right], \tag{34}$$

where we have used the symmetry properties of the real and imaginary parts of the dielectric function $\epsilon(k,\omega)$ from Eq. (26). We note that the stopping force is the negative of the usual stopping power, $F_s = -S$, whereas the image force is related to the familiar image potential of an ion by $F_i = -dV_i/dz_0$.[32]

Because the main parameters characterizing the system are the ground-state charge carrier density n_0 (and, through it, the gating voltage V_g) and the temperature, it appears most rational to use the TF inverse screening length k_{TF}, defined in Eq. (27), as a scaling parameter to express our results in dimensionless form. So, we first change ω to $\Omega = \omega/(kv_F)$ in Eqs. (33) and (34) to reflect the fact that the functions $\mathcal{X}_r$ and $\mathcal{X}_i$ in Eqs. (24) and (25) are universal functions of Ω, and then we change k to $K = k/k_{\mathrm{TF}}$. This enables us to express the reduced stopping and image forces, $\bar{F}_s = F_s/(Qk_{\mathrm{TF}})^2$ and $\bar{F}_i = F_i/(Qk_{\mathrm{TF}})^2$, as functions of the reduced ion distance $\bar{z}_0 = z_0 k_{\mathrm{TF}}$ and the reduced ion speed $\bar{v} = v/v_F$, as follows:

$$\bar{F}_s = \frac{2}{\pi}\frac{1}{\bar{v}}\int_0^\infty dK K e^{-2K\bar{z}_0}\int_0^{\bar{v}} d\Omega \frac{\Omega}{\sqrt{\bar{v}^2 - \Omega^2}}\,\mathrm{Im}\left[\frac{1}{\epsilon(K,\Omega;\bar{\gamma},\bar{h})}\right], \tag{35}$$

$$\bar{F}_i = \frac{2}{\pi}\int_0^\infty dK K e^{-2K\bar{z}_0}\int_0^{\bar{v}} \frac{d\Omega}{\sqrt{\bar{v}^2 - \Omega^2}}\,\mathrm{Re}\left[\frac{1}{\epsilon(K,\Omega;\bar{\gamma},\bar{h})} - 1\right]. \tag{36}$$

Here, we have indicated that the remaining dependencies on the graphene parameters are retained in the dielectric function via the reduced graphene-substrate gap $\bar{h} = hk_{\mathrm{TF}}$ appearing in ϵ_0, as defined in Eq. (9), and the reduced decay constant $\bar{\gamma} = \gamma/(k_{\mathrm{TF}}v_F)$ which is defined so that the universal dependencies on $\Gamma = \gamma/(kv_F)$ in Eqs. (24) and (25) are retained by writing $\Gamma = \bar{\gamma}/K$. It is particularly gratifying to note that, in the usual collisionless and zero-gap cases of the RPA treatments of screening by graphene,[7,10,12] the expressions for the reduced forces [Eqs. (35) and (36)] become universal functions of the reduced distance $\bar{z}_0$ and the reduced speed $\bar{v}$, thereby covering wide ranges of temperature and the gate voltage. As a reference, we note that, for the density of $n_0 = 10^{12}$ cm^{-2} which is typically achieved in gated graphene, one obtains at zero temperature $k_{\mathrm{TF}} \approx 0.16$ Å^{-1}. Moreover, as the graphene-substrate gap may be estimated to be at least on the order of the van der Waals radius of a carbon atom, 1.7 Å, or even about twice that amount in the case of a SiO_2 substrate,[29] one can then estimate the typical value of the reduced gap to be $\bar{h} \sim 0.5$. As for the relaxation time, one can use the experimental values for the electron mean free paths in graphene to estimate τ to be as large as 3×10^{-13} s^{-1}, giving $\bar{\gamma} \sim 0.21 \times 10^{-3}$ or more, depending on the density of impurities.[4]

In Fig. 1, we show the velocity dependencies of the (a) stopping and (b) image forces for three values of the gap $\bar{h}$ between graphene and a SiO_2 substrate, with fixed $\bar{z}_0 = 1$ and $\bar{\gamma} = 0$. One notices almost linear increase in the stopping force at low speeds due to the intraband single-electron excitations, followed by a massive peak after the speed $\bar{v} = 1$ which is a threshold for energy loss to the plasmon excitations, and a slow decrease in stopping force at the higher speeds. We note that the high-speed behavior may be somewhat changed in the presence of the interband electron transitions and the corresponding plasmon decay. The image force shows similar resonant features at around the speed $\bar{v} = 1$ with the significant tendency of saturation at the lowest and the highest speeds shown. However, the most remarkable features shown in Fig. 1 are the very strong dependencies of both forces on values of the graphene-substrate gap, with $\bar{h} = \infty$ standing for a free graphene, $\bar{h} = 0$ being the zero-gap approximation employed in the RPA studies of graphene screening, whereas $\bar{h} = 0.5$ is probably close to a typical experimental situation. In Fig. 2, we show the dependencies of the stopping and image forces on the ion-graphene distance $\bar{z}_0$ for the same three values of the gap $\bar{h}$, as in Fig. 1, and for two typical speeds, $\bar{v} = 0.5$ and 1.5, straddling the plasmon threshold at $\bar{v} = 1$, with $\bar{\gamma} = 0$. One notices an overall decay in magnitudes of both forces which are, given the logarithmic scale, again strongly affected by the value of $\bar{h}$. One also notices that both forces diverge as $\bar{z}_0 = z_0 k_{\mathrm{TF}} \to 0$, which can be traced back to the failure of the linear response theory for point

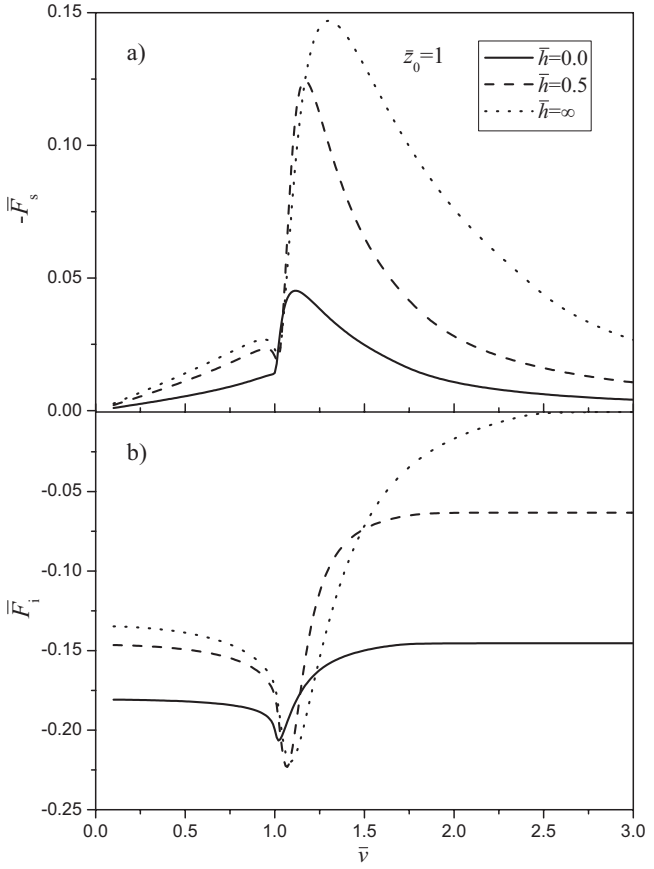

FIG. 1. The reduced (a) stopping and (b) image forces as functions of the reduced speed $\bar{v}$ for an ion moving at the reduced distance $\bar{z}_0=1$ above graphene for three values of the reduced gap between graphene and a SiO_2 substrate, $\bar{h}=0.0$ (solid lines), 0.5 (dashed lines), and ∞ (dotted lines), with zero damping, $\bar{\gamma}=0$.

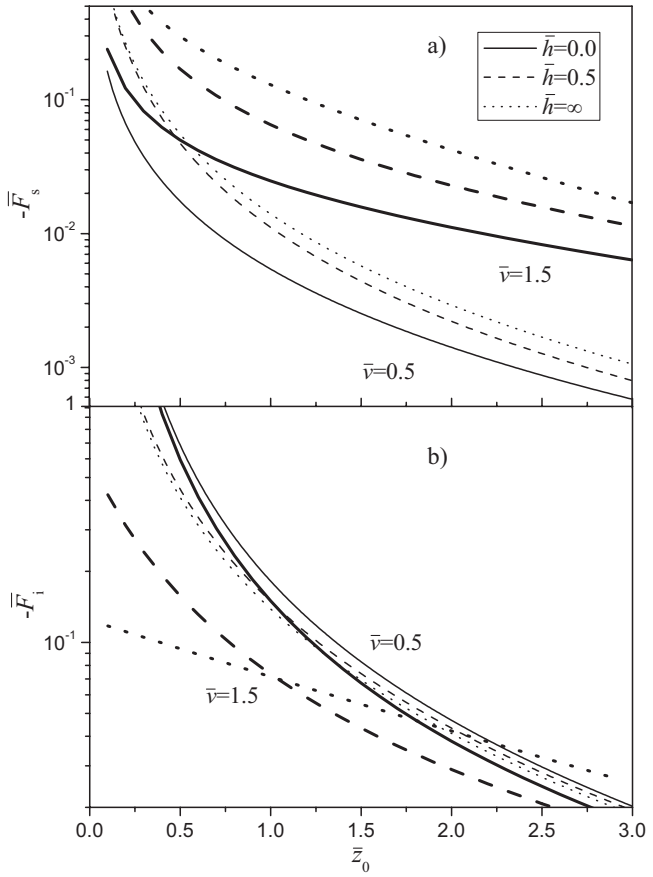

FIG. 2. The reduced (a) stopping and (b) image forces as functions of the reduced distance $\bar{z}_0$ above graphene for an ion moving at two values of the reduced speed, $\bar{v}=0.5$ (thin lines) and 1.5 (thick lines), and for three values of the reduced gap between graphene and a SiO_2 substrate, $\bar{h}=0.0$ (solid lines), 0.5 (dashed lines), and ∞ (dotted lines), with zero damping, $\bar{\gamma}=0$.

charges in intrinsic graphene, because $k_{\mathrm{TF}} \propto \sqrt{|n_0|} \to 0$ for vanishing gate voltage from Eq. (12).[7] For extrinsic graphene, those divergencies may be remedied when the interband electron transitions are included.

In order to further explore the effect of the graphene-substrate gap, we show in Fig. 3 the $\bar{h}$ dependencies of both forces for three speeds $\bar{v}$, with fixed $\bar{z}_0=1$ and $\bar{\gamma}=0$. One notices the remarkably strong dependencies in the range of small gaps, say $\bar{h}<1$, with a very slow leveling toward large $\bar{h}$ values, which may even occur in a nonmonotonous manner as shown for the image force at the speed $\bar{v}=1.5$ in Fig. 3(b). Since $\bar{h}\sim 0.5$ is likely close to a realistic value, one may conclude that any uncertainty or spatial variation of the gap size in directions across graphene may bring relatively large fluctuations in the values of both the stopping and image forces on moving ions.[29] Finally, in Fig. 4, we choose $\bar{h}=0.5$ to illustrate the effects of a finite decay constant $\bar{\gamma}$ on the velocity dependencies of the stopping and image forces for fixed $\bar{z}_0=1$. As expected, one notices the effect of smoothing out the resonant features in both forces around the speed $\bar{v}=1$, with little influences on their high-speed behaviors and on the low-speed behavior of the stopping force. However, the low-speed values of the image force are noticeably dependent on $\bar{\gamma}$, indicating that, when studying static screening of charged impurities,[3–6] the dielectric function [Eq. (32)] would likely give different results in comparison to the linear TF model [Eq. (31)].

It is of particular interest for the interactions of slow charges with graphene to obtain analytical expressions for the image and stopping forces for vanishing projectile speed v. This can be achieved by assuming $\gamma=0$ and $\epsilon_0=\mathrm{const}$, so that one obtains a stopping force which is proportional to the ion speed, $\bar{F}_s=-\eta\bar{v}$, with the friction coefficient η given by

$$\eta=\frac{1}{2\epsilon_0^3}\left[\frac{1}{\zeta}+1-(2+\zeta)e^{\zeta}\,\mathrm{Ei}(1,\zeta)\right], \tag{37}$$

and the static image force given by

$$\bar{F}_i=\frac{1}{\epsilon_0^3}\left[\frac{1-\epsilon_0}{\zeta^2}-\frac{1}{\zeta}+e^{\zeta}\,\mathrm{Ei}(1,\zeta)\right], \tag{38}$$

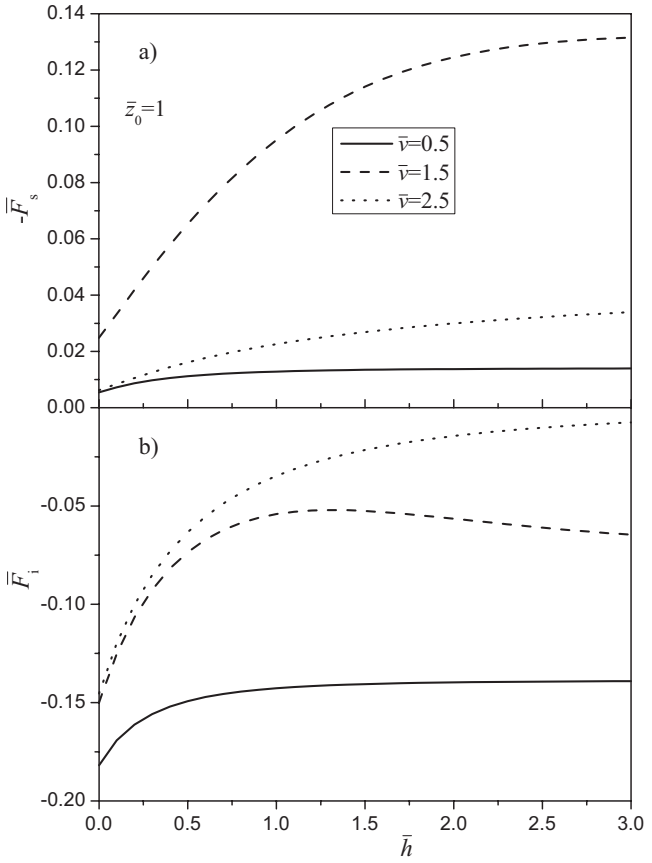

FIG. 3. The reduced (a) stopping and (b) image forces as functions of the reduced gap $\bar{h}$ between graphene and a SiO_2 substrate, for an ion moving at the reduced distance $\bar{z}_0=1$ above graphene, with three values of the reduced speed, $\bar{v}=0.5$ (solid lines), 1.5 (dashed lines), and 2.5 (dotted lines), and with zero damping, $\bar{\gamma}=0$.

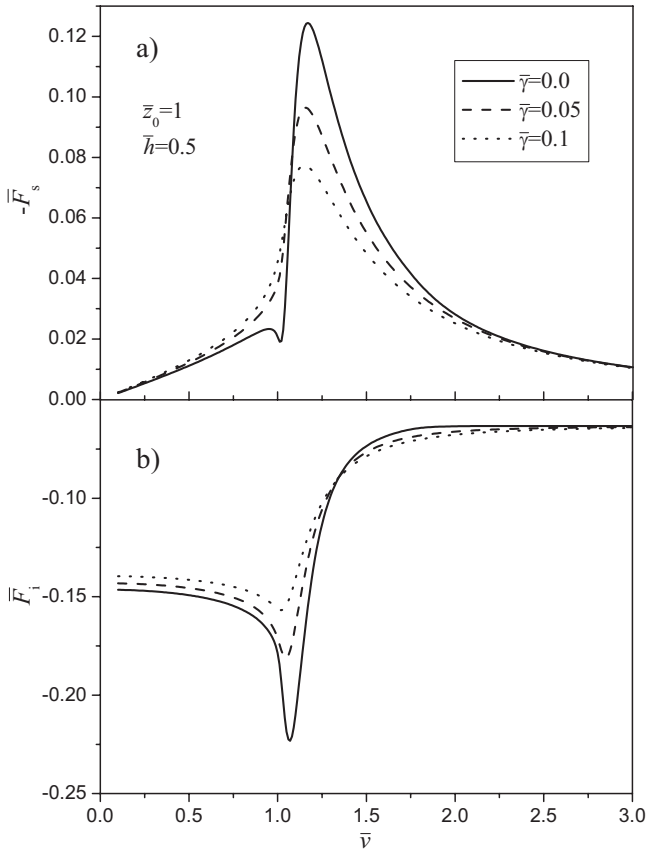

FIG. 4. The reduced (a) stopping and (b) image forces as functions of the reduced speed $\bar{v}$ for an ion moving at the reduced distance $\bar{z}_0=1$ above graphene for three values of the reduced damping, $\bar{\gamma}=0$ (solid lines), 0.05 (dashed lines), and 0.1 (dotted lines), with the reduced gap between graphene and a SiO_2 substrate being $\bar{h}=0.5$.

where $\zeta \equiv 2\bar{z}_0/\epsilon_0$ and $\mathrm{Ei}(1,\zeta)$ is the standard exponential integral.[35] Note that the leading term in the asymptotic expansion of the image force at large distances for graphene in free space ($\epsilon_0=1$) gives $F_i \sim -Q^2/(4z_0^2)$, typical for a perfectly conducting surface.

IV. CONCLUDING REMARKS

We have used a semiclassical model based on the Vlasov equations to describe the dynamic polarization of graphene's π electrons under the gating conditions in response to slowly moving charges, with a particular attention paid to the effects of temperature, electron scattering, and the size of the gap h between graphene and substrate. We have obtained expressions for the stopping force and the image force on point charges moving parallel to graphene in which the effects of variations in both temperature and gate voltage are included through a TF inverse screening length as a single scaling parameter, whereas the decay rate due to electron scattering and the graphene-substrate gap were examined as external parameters. We have found sizable effects of the decay rate, especially around the threshold ion speed for plasmon excitations, $v \approx v_F$. The most dramatic and the most important among our findings is that the size of the graphene-substrate gap h may exert quite large influence on the magnitudes of the dynamic-polarization forces on moving ions and, in particular, that the rates of change with h in these effects are the largest in the range of h values compatible with the experimental data for supported graphene. Therefore, given that the standard deviation of the gap size h was found experimentally to be large compared to its mean value for graphene lying on a SiO_2 substrate,[29] one may expect substantial variations in both the stopping and image forces on ions traversing large areas across such systems.

Finally, we have shown how a nonlinear model for static screening arises from the steady-state solutions of the Vlasov equations. Given that the linear theory of screening was shown to completely fail in the case of intrinsic graphene,[7] we shall attempt in future work to implement the nonlinear kinetic model to derive both the image force and the friction coefficient for slow charges moving over a supported graphene with small or zero gate voltage. Other improvements will include an analysis of the effects of the interband electron transitions on the dynamic-polarization forces on ions moving at the intermediate speeds.

ACKNOWLEDGMENTS

The authors are grateful to N. Bibic for insightful discussions and continuing support. This work has been supported by the Ministry of Science, Republic of Serbia. Z.L.M. also acknowledges support by the Natural Sciences and Engineering Research Council of Canada.

APPENDIX: NONLINEAR THOMAS–FERMI MODEL OF STATIC SCREENING

In this Appendix, we demonstrate how a temperature-dependent, self-consistent model for nonlinear screening of a static external charge arises from the Vlasov equations [Eq. (17)].[7] We shall assume a point charge Q at the position $z_0 \geqslant -h$, so that cases of charged impurities lying between the graphene and the substrate surface ($-h \leqslant z_0 < 0$) can be studied, in addition to the charges lying on the upper side of graphene ($z > 0$).

Using the Fourier transform with respect to coordinates in the graphene plane, $\mathbf{r} \to \mathbf{k}$, the total (screened) potential from Eq. (1) can be expressed via Eqs. (3)–(5) as follows:

$$\tilde{\Phi}(\mathbf{k},z) = \frac{2\pi}{k}[Qe^{-k|z-z_0|} + \tilde{\sigma}_{\mathrm{gr}}(\mathbf{k})e^{-k|z|} + \tilde{\sigma}_{\mathrm{sub}}(\mathbf{k})e^{-k|z+h|}]. \tag{A1}$$

Next, one can use this expression to obtain $\tilde{\sigma}_{\mathrm{sub}}$ from the boundary condition [Eq. (2)] as follows:

$$\tilde{\sigma}_{\mathrm{sub}}(\mathbf{k}) = -\frac{\epsilon_{\mathrm{sub}}-1}{\epsilon_{\mathrm{sub}}+1}[\tilde{\sigma}_{\mathrm{gr}}(\mathbf{k}) + Qe^{-kz_0}]e^{-kh}, \tag{A2}$$

which, upon substitution back into Eq. (A1), allows one to write the inverse Fourier transform, $\mathbf{k} \to \mathbf{r}$, of the total potential in the system, $\Phi(\mathbf{r},z)$, in terms of an integral over the charge density (per unit area), $\sigma_{\mathrm{gr}}(\mathbf{r}) = -en_{\mathrm{gr}}(\mathbf{r})$, induced on graphene by the external point charge,

$$\begin{aligned}\Phi(\mathbf{r},z) = Q\Bigg[&\frac{1}{\sqrt{r^2+(z-z_0)^2}} \\ &- \frac{\epsilon_{\mathrm{sub}}-1}{\epsilon_{\mathrm{sub}}+1}\frac{1}{\sqrt{r^2+(z_0+h+|z+h|)^2}}\Bigg] \\ &- e\int d^2\mathbf{r}' n_{\mathrm{gr}}(\mathbf{r}')\Bigg[\frac{1}{\sqrt{(\mathbf{r}-\mathbf{r}')^2+z^2}} \\ &- \frac{\epsilon_{\mathrm{sub}}-1}{\epsilon_{\mathrm{sub}}+1}\frac{1}{\sqrt{(\mathbf{r}-\mathbf{r}')^2+(h+|z+h|)^2}}\Bigg].\end{aligned} \tag{A3}$$

We note that the terms in this expression involving the factor $(\epsilon_{\mathrm{sub}}-1)/(\epsilon_{\mathrm{sub}}+1)$ describe the contributions of the classical image of charges in the substrate.

To proceed further, one needs to deal with the values of the total electric potential in the graphene plane, which we denote as

$$\phi(\mathbf{r}) \equiv \Phi(\mathbf{r},z)|_{z=0}. \tag{A4}$$

In passing, we note that $\phi(\mathbf{r})$ is precisely the potential required in calculations of the electron transport in graphene based on some sort of a two-dimensional scattering formalism.[3–6] Next, note that the ground state of the system with a static point charge is described by the steady-state solution of the Vlasov equations [Eq. (17)] in the local form, $f_{\pm}(\mathbf{p},\mathbf{r}) = f_{\pm}^0(\mathbf{p},\mathbf{r}) = f[\varepsilon_{\pm}(\mathbf{p}) - e\phi(\mathbf{r})]$, where $f(\varepsilon)$ is the Fermi-Dirac distribution [Eq. (15)]. This allows one to evaluate n_{gr} from Eq. (20) as follows:

$$n_{\mathrm{gr}}(\mathbf{r}) = n_0[\mu + e\phi(\mathbf{r})] - n_0(\mu), \tag{A5}$$

where $n_0(\mu)$ is given by Eq. (16). Now, by setting $z=0$ in Eq. (A3) and using $n_{\mathrm{gr}}(\mathbf{r}')$ from Eq. (A5), one obtains the following nonlinear integral equation for $\phi(\mathbf{r})$:

$$\begin{aligned}\phi(\mathbf{r}) = Q&\left[\frac{1}{\sqrt{r^2+z_0^2}} - \frac{\epsilon_{\mathrm{sub}}-1}{\epsilon_{\mathrm{sub}}+1}\frac{1}{\sqrt{r^2+(z_0+2h)^2}}\right] \\ &- e\int d^2\mathbf{r}'\{n_0[\mu + e\phi(\mathbf{r}')] - n_0(\mu)\} \\ &\times\left[\frac{1}{\|\mathbf{r}-\mathbf{r}'\|} - \frac{\epsilon_{\mathrm{sub}}-1}{\epsilon_{\mathrm{sub}}+1}\frac{1}{\sqrt{(\mathbf{r}-\mathbf{r}')^2+4h^2}}\right].\end{aligned} \tag{A6}$$

Once Eq. (A6) is solved for the values of the screened potential $\phi(\mathbf{r})$ in the graphene plane, one can obtain $n_{\mathrm{gr}}(\mathbf{r}')$ from Eq. (A5) and use it in Eq. (A3) to finally calculate the screened potential throughout the space and, in particular, to evaluate the image potential of the external charge from $V_i(z_0) = Q\Phi_{\mathrm{ind}}(\mathbf{r}=0,z_0)$, where $\Phi_{\mathrm{ind}}(\mathbf{r},z)$ is given by Eq. (A3) without the first term. Finally, we mention that a similar procedure can be repeated for charges embedded in the substrate, $z_0 < -h$.

Of course, if the potential $\phi(\mathbf{r})$ is weak enough, one can linearize n_{gr} in Eq. (A3), $n_{\mathrm{gr}}(\mathbf{r}') \approx e\phi(\mathbf{r}')\frac{\partial n_0}{\partial \mu}$, with $n_0(\mu)$ given by Eq. (16), solve the resulting equation for $\phi(\mathbf{r})$ by using the Fourier transform, and end up with a linear screening model based on the TF dielectric function [Eq. (31)].

*zmiskovi@math.uwaterloo.ca

[1] K. S. Novoselov, A. K. Geim, S. V. Morozov, D. Jiang, Y. Zhang, S. V. Dubonos, I. V. Grigorieva, and A. A. Firsov, Science **306**, 666 (2004).

[2] K. S. Novoselov, A. K. Geim, S. V. Morozov, D. Jiang, M. I. Katsnelson, I. V. Grigorieva, S. V. Dubonos, and A. A. Firsov, Nature (London) **438**, 197 (2005).

[3] T. Ando, J. Phys. Soc. Jpn. **75**, 074716 (2006).

[4] N. M. R. Peres, J. M. B. Lopes dos Santos, and T. Stauber, Phys. Rev. B **76**, 073412 (2007); T. Stauber, N. M. R. Peres, and F. Guinea, *ibid.* **76**, 205423 (2007).

[5] E. H. Hwang, S. Adam, and S. Das Sarma, Phys. Rev. Lett. **98**,

186806 (2007); S. Adam, E. H. Hwang, V. M. Galiskii, and S. Das Sarma, Proc. Natl. Acad. Sci. U.S.A. **104**, 18392 (2007).
[6] E. G. Mishchenko, Phys. Rev. Lett. **98**, 216801 (2007).
[7] M. I. Katsnelson, Phys. Rev. B **74**, 201401(R) (2006).
[8] M. I. Katsnelson, Mater. Today **10**, 20 (2007).
[9] W. L. Barnes, A. Dereux, and T. W. Ebbesen, Nature (London) **424**, 824 (2003); E. Ozbay, Science **311**, 189 (2006).
[10] B. Wunsch, T. Stauber, F. Sols, and F. Guinea, New J. Phys. **8**, 318 (2006).
[11] O. Vafek, Phys. Rev. Lett. **97**, 266406 (2006).
[12] E. H. Hwang and S. Das Sarma, Phys. Rev. B **75**, 205418 (2007).
[13] L. Brey and H. A. Fertig, Phys. Rev. B **75**, 125434 (2007).
[14] X.-F. Wang and T. Chakraborty, Phys. Rev. B **75**, 033408 (2007).
[15] V. Ryzhii, A. Satou, and T. Otsuji, J. Appl. Phys. **101**, 024509 (2007).
[16] F. Rana, IEEE Trans. Nanotechnol. **7**, 91 (2008).
[17] I. Radovic, Lj. Hadzievski, N. Bibic, and Z. L. Miskovic, Phys. Rev. A **76**, 042901 (2007).
[18] M. Khantha, N. A. Cordero, L. M. Molina, J. A. Alonso, and L. A. Girifalco, Phys. Rev. B **70**, 125422 (2004).
[19] S. Tomassone and A. Widom, Phys. Rev. B **56**, 4938 (1997).
[20] G. V. Dedkov and A. A. Kyasov, Nucl. Instrum. Methods Phys. Res. B **237**, 507 (2005).
[21] H. H. Brongersma, M. Draxler, M. de Ridder, and P. Bauer, Surf. Sci. Rep. **62**, 63 (2007).
[22] A. V. Krasheninnikov and K. Nordlund, Phys. Rev. B **71**, 245408 (2005); C. S. Moura and L. Amaral, J. Phys. Chem. B **109**, 13515 (2005); W. Zhang, Z. Zhu, Z. Xu, Z. Wang, and F. Zhang, Nanotechnology **16**, 2681 (2005); Z. L. Miskovic, Radiat. Eff. Defects Solids **162**, 185 (2007).
[23] G. Ramos and B. M. U. Scherzer, Nucl. Instrum. Methods Phys. Res. B **85**, 479 (1995); **174**, 329 (2001).
[24] E. Yagi, T. Iwata, T. Urai, and K. Ogiwara, J. Nucl. Mater. **334**, 9 (2004).
[25] S. Cernusca, M. Fürsatz, H. P. Winter, and F. Aumayr, Europhys. Lett. **70**, 768 (2005).
[26] H. Winter, Phys. Rep. **367**, 387 (2002).
[27] J. Burgdörfer, P. Lerner, and F. W. Meyer, Phys. Rev. A **44**, 5674 (1991).
[28] G. Bertoni, L. Calmels, A. Altibelli, and V. Serin, Phys. Rev. B **71**, 075402 (2005).
[29] M. Ishigami, J. H. Chen, W. G. Cullen, M. S. Fuhrer, and E. D. Williams, Nano Lett. **7**, 1643 (2007).
[30] D. J. Mowbray, Z. L. Miskovic, and F. O. Goodman, Phys. Rev. B **74**, 195435 (2006).
[31] E. Prodan, C. Radloff, N. J. Halas, and P. Nordlander, Science **302**, 419 (2003).
[32] J. M. Pitarke, V. M. Silkin, E. V. Chulkov, and P. M. Echenique, Rep. Prog. Phys. **70**, 1 (2007).
[33] N. D. Mermin, Phys. Rev. B **1**, 2362 (1970).
[34] T. P. Doerr and Y. K. Yu, Am. J. Phys. **72**, 190 (2004).
[35] M. Abramowitz and I. A. Stegun, *Handbook of Mathematical Functions*, (National Bureau of Standards, Washington, 1965).